Decay of a $2p$ Inner-Shell Hole in an Ar^+ Ion

S.-M. Huttula,[1] P. Lablanquie,[2,3] L. Andric,[2,3,8] J. Palaudoux,[2,3] M. Huttula,[1]
S. Sheinerman,[4] E. Shigemasa,[5] Y. Hikosaka,[6] K. Ito,[7] and F. Penent[2,3]

[1]*Department of Physics, University of Oulu, P.O. Box 3000, 90014 Oulu, Finland*
[2]*UPMC, Université Paris 06, LCPMR, 11 rue Pierre et Marie Curie, 75231 Paris Cedex 05, France*
[3]*CNRS, LCPMR (UMR 7614), 11 rue Pierre et Marie Curie, 75231 Paris Cedex 05, France*
[4]*Department of Physics, St. Petersburg State Maritime Technical University, 198262 St. Petersburg, Russia*
[5]*UVSOR Facility, Institute for Molecular Science, Okazaki 444-8585, Japan*
[6]*Department of Environmental Science, Niigata University, Niigata 950-2181, Japan*
[7]*Photon Factory, Institute of Materials Structure Science, Oho, Tsukuba 305-0801, Japan*
[8]*Université Paris-Est, F77454 Marne La Vallee 2, France*

(Received 16 November 2012; published 12 March 2013)

Direct measurements of the photoelectrons or Auger electrons associated with inner shell ionization of positively charged ions are extremely difficult and rarely realized. We propose an alternative method to simulate such measurements, based on core valence double photoionization of the neutral species. As an example, we obtain the spectroscopy, lifetimes, and Auger decays of the states arising from $2p$ inner shell ionisation of an Ar^+ ion. Observations compare well with theoretical predictions obtained within multiconfigurational Dirac-Fock formalism.

DOI: 10.1103/PhysRevLett.110.113002 PACS numbers: 32.80.Fb, 31.15.ag, 32.80.Hd

Knowledge of the inner-shell photoionization of atomic ions is of fundamental interest and an important ingredient to model astrophysical and laboratory plasmas. Absolute inner-shell photoionization cross sections and properties of inner-shell resonances (such as their spectroscopy and lifetime) have been obtained experimentally from ion detection techniques and serve to test existing models [1]. Recent targets include C^{3+} [2], B^{2+} [3], N^+ [4], and Ar^{n+} [5]. However, the inner-shell electronic properties of ions are still largely unexplored, because experiments succeeding in measuring directly electron spectra from positive ions are extremely difficult and rarely performed. This is due to the very low density available in ionic beams, compared to the photon flux offered at synchrotron centers, and the high background due to the high collisional cross sections involving ions. Although the advent of the much more intense XFEL sources will certainly improve the situation, a new experimental method for observing electron spectroscopy of ions would be helpful. In fact, to the best of our knowledge, the only results reported up to now present a photoelectron spectra arising from $4d$ ionization of the Xe^+ ion [6] and resonant Auger spectra associated with the decay of intense $3p$ resonances in Ca^+ [7–9].

In this Letter we present an alternative method to obtain photoelectron and Auger electron spectroscopy of positively charged ions. It is based on the single photon multi-ionization of the corresponding neutral atom and on coincidence techniques. As a proof of principle, we demonstrate that core-valence double ionization of the Ar atom allows us to deduce the spectroscopy of the $2p$ holes in an Ar^+ ion. A number of states are observed, reflecting the different possible couplings of the $2p$ hole with the valence ($3p$ or $3s$) hole. These states decay by Auger electron emission and for each of them, the associated lifetime and Auger electron spectra are obtained. Theoretical calculations for the transitions are obtained using multiconfigurational Dirac-Fock (MCDF) formalism.

Experiments were mainly performed on the U56/2 PGM1 beam line of the BESSY-II synchrotron during single bunch operation. We used our magnetic bottle time-of-flight analyzer HERMES (High Energy Resolution Multi Electron Spectrometer), which has been described in detail before [10,11]. Briefly, HERMES allows the simultaneous collection of almost all electrons ($> 95\%$ of the 4π solid angle) emitted following ionization of a single atom. The high detection efficiency ($50 \pm 5\%$ for 0–300 eV electrons) leads to efficient multicoincidence experiments. The energy resolution of the apparatus, $\Delta E/E$, was found to be nearly constant at 1.5% for electrons of $E > 1$ eV, though ΔE was limited to around 20 meV (FWHM) for $E < 1$ eV. A multielectron coincidence data set was accumulated at 334.3 eV photon energy with a photon bandwidth set to 30 meV. Complementary experiments were conducted at the undulator beam line BL-16A of the Photon Factory. The experimental setup is a magnetic bottle type analyzer similar to the one used in experiments at BESSY and was described previously [12]. These complementary experiments were conducted at lower photon energies in order to observe the photoelectron lines associated with $2p$ shell ionization with higher resolution.

The experimental method to retrieve electron spectra that would result from the formation and decay of a $2p$ inner-shell hole in an Ar^+ ion is illustrated in Fig. 1. A photon energy of $h\nu = 334.3$ eV is used to induce

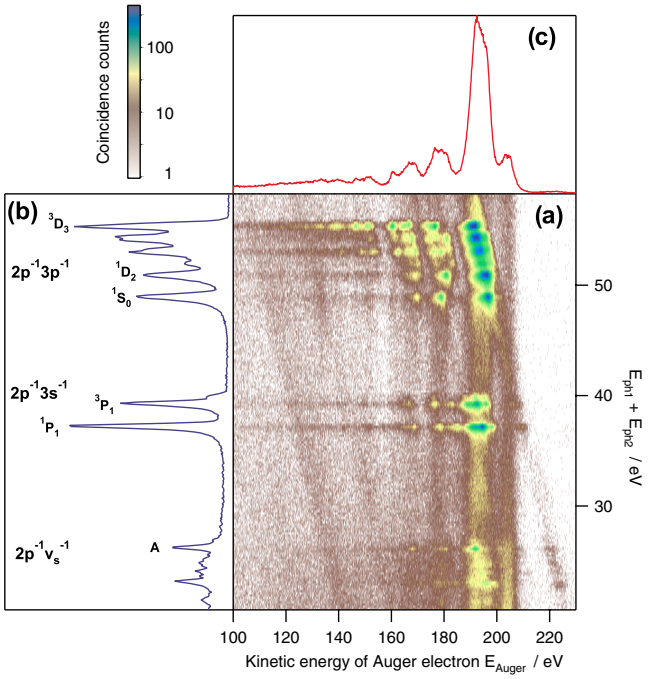

FIG. 1 (color online). (a) Energy correlations among three electrons detected in coincidence upon triple ionization of Ar atoms with 334.3 eV photons. They are represented as a function of the sum of the two slower electron energies (y axis) and of the faster one (x axis). The projections of the two-dimensional coincidence map reveal the Ar^{2+} $2p^{-1}v^{-1}$ intermediate states in (b) and their Auger decay in (c). To reduce background, the slowest electron is imposed to lie between 4 and 10 eV, a region where the $2s$ photoelectron is expected [11].

core-valence double ionization of Ar atoms, producing Ar^{2+} $2p^{-1}v^{-1}$ states that further decay by Auger electron emission to form Ar^{3+} v^{-3} final states ($v = 3s$ or $3p$). The process is the following:

$$h\nu + \mathrm{Ar} \rightarrow \mathrm{Ar}^{2+}2p^{-1}v^{-1} + e_{\mathrm{ph1}} + e_{\mathrm{ph2}} \quad (1a)$$

$$\rightarrow \mathrm{Ar}^{3+}v^{-3} + e_{\mathrm{Auger}}. \quad (1b)$$

This process is isolated from the dominant $2p$ inner-shell photoionization path by the detection in coincidence of the three released electrons (the two photoelectrons $e_{\mathrm{ph1,2}}$ and the Auger electron e_{Auger}). The coincidence counts are reported in Fig. 1(a) as a function of the Auger energy (x axis) and of the sum of the photoelectron energies $E_{\mathrm{ph1}} + E_{\mathrm{ph2}}$ (y axis). It is seen from Eq. (1a) that the histogram $E_{\mathrm{ph1}} + E_{\mathrm{ph2}}$ [Fig. 1(b)] defines the Ar^{2+} $2p^{-1}v^{-1}$ core valence states. These states have been described previously [11] and include states where the valence hole is $3p^{-1}$, $3s^{-1}$ or a "satellite valence hole" v_s^{-1} (this denomination is used here to describe a configuration such as $3p^{-2}nl$ where a valence electron is ionized and a second valence electron is simultaneously excited). These Ar^{2+} $2p^{-1}v^{-1}$ states are exactly the same states as would be formed by $2p$ inner shell ionization of an Ar^{+} v^{-1} ion, although their relative populations will differ in the two formation paths.

The Auger spectra associated with the decay of each Ar^{2+} $2p^{-1}v^{-1}$ state appears then in the horizontal coincidence lines of Fig. 1(a). Representative Auger spectra of selected Ar^{2+} $2p^{-1}v^{-1}$ states are extracted by plotting the coincidence counts along the corresponding lines (Auger spectra of all $2p^{-1}v^{-1}$ states are reported in the supplemental appendix [13]). They are reported in Fig. 2, and compared to the Auger spectra associated with the decay of a $2p_{1/2}$ or $2p_{3/2}$ hole in neutral Ar. These Auger decays have been observed previously [14], but could not be isolated individually, because of the lack of a coincidence method. A striking remark is that the main Auger components associated with the decay of a $2p$ hole in an Ar^{+} ion appear at ~195 eV Auger electron kinetic energy, that is some 10 eV lower than the main Auger peak due to the decay of a $2p$ hole in a neutral Ar atom. This holds true whether the valence hole is a $3p^{-1}$, a $3s^{-1}$ or even a satellite valence hole v_s^{-1}. This property can have a practical application. Auger spectroscopy is known to be element specific and is widely used to identify material composition; we show here that it is also sensitive to the charge of the element, which could be useful, for instance, in plasma diagnostics.

In order to understand why the main Auger peaks have similar energies, whatever the initial Ar^{2+} $2p^{-1}v^{-1}$ state, we have calculated the associated Auger spectra. Calculations were conducted to describe the Ar^{2+} $2p^{-1}v^{-1}$ initial states, the Ar^{3+} v^{-3} final states reached in the Auger decay, and the associated transition probabilities. The calculations were carried out using the MCDF formalism by applying the GRASP92 code [15] and the RELCI extension [16]. The MCDF method is described in detail elsewhere (see, e.g., Ref. [15] and references therein), thereby only the main principles are reviewed here. In the

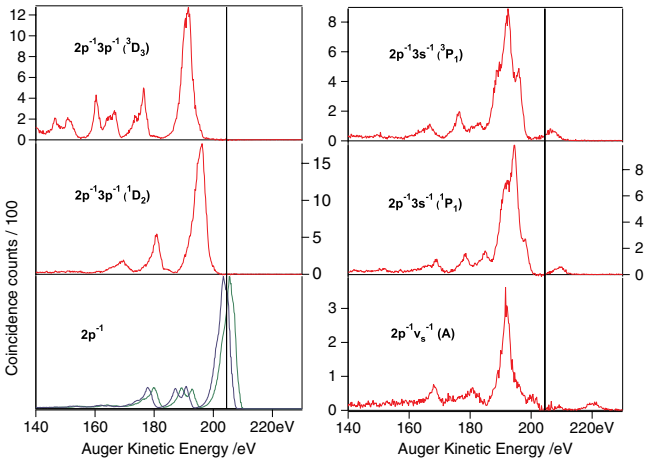

FIG. 2 (color online). Auger spectra associated with the decay of selected Ar^{2+} $2p^{-1}v^{-1}$ states (red). They are deduced from the coincidence counts along the horizontal lines of Fig. 1(a) and compared with the Auger decay of a simple $2p_{3/2}$ (blue) or $2p_{1/2}$ (green) hole. These last two Auger spectra are obtained in the same data set from coincidences between the $2p$ photoelectrons and the associated Auger electrons.

MCDF method, the atomic state functions (ASFs), characterized by the total angular momentum J_α and parity P_α, are represented in the basis of the jj-coupled configuration state functions (CSFs) with the same J_α and parity P_α, as

$$|\Psi_\alpha(P_\alpha J_\alpha)\rangle = \sum_k c_{\alpha k} |\psi_k(P_\alpha J_\alpha)\rangle.$$

The mixing coefficients $c_{\alpha k}$ are obtained by diagonalizing the two-electron interaction matrix, which allows one to take the electronic correlations into account. The wave functions are obtained self-consistently using the Dirac-Coulomb Hamiltonian.

For the light mass of Ar, the orbital and spin angular momenta of the outer electrons are not strongly interacting. Therefore, the coupling conditions are closer to the LSJ coupling. Thus for the analysis the inherently jj-coupled ASFs were transformed into the LSJ basis by the unitary transform between the two bases applying the program LSJ [17].

The Auger decay intensity is given by

$$n_{f\beta} = \frac{2\pi \sum_{l_{A j_A}} |\sum_{\mu\nu} c_{f\mu} c_{\beta\nu} M^{\mu\nu}_{f\beta}(J_f, J_\beta)|^2}{P_\beta(J_\beta)} Q_\beta(J_\beta),$$

where $M^{\mu\nu}_{f\beta}(J_f, J_\beta)$ is the Coulomb matrix element $\langle \psi_\mu(J_f) \epsilon_A l_A j_A; J_\beta || \sum_{mn}^{N-1} 1/r_{mn} || \psi_\nu(J_\beta) \rangle$, $P_\beta(J_\beta)$ is the total decay rate, and $Q_\beta(J_\beta)$ is the $|\Psi(J_i)\rangle \rightarrow |\Psi(J_\beta)\rangle$ ionization cross section. In the equation, $|\Psi(J_i)\rangle$, $\Psi(J_\beta)\rangle$ and $|\Psi(J_f)\rangle$ represent the ground state, ionized state, and Auger final state of the atom, respectively. Channel interactions were omitted in our calculations. In Ar L_3MM Auger transitions [18], their effects have been reported to be minor due to the relatively large Auger electron energies. The Auger decay intensities were calculated with the AUGER component from the RATIP package [19].

We have compared the results of calculations to the experimental spectra in Fig. 3. They are represented as a function of the binding energies E_b of the Ar^{3+} final states. Agreement between calculations and experiment is excellent: the partly resolved structure of the main Auger peaks is well reproduced. Three groups of final states are distinguished, with configurations $3p^{-3}$ at $E_b \sim 85$ eV (with its ^4S, ^2P and ^2D components), $3s^{-1}3p^{-2}$ at $E_b \sim 100$ eV, and $v_s^{-1}3p^{-2}$ for $E_b < 110$ eV. It is seen that these groups are populated preferentially by the decay of $2p^{-1}3p^{-1}$, $2p^{-1}3s^{-1}$, and $2p^{-1}v_s^{-1}$ states, respectively. This can be summarized by saying that a $2p$ hole decays preferentially by involving two $3p$ electrons, and that if the decay occurs in the presence of a valence hole, this valence hole remains a spectator of the decay, leading to similar Auger energies of ~195 eV.

The lifetime of a $2p$ hole in neutral Argon amounts to 5.5 fs, corresponding to a energy broadening of 118 meV [20]. Our calculations reported in Table I predict that the lifetime of a $2p$ hole in an Ar^+ ($3p^{-1}$) ion can differ by more than an order of magnitude depending on the

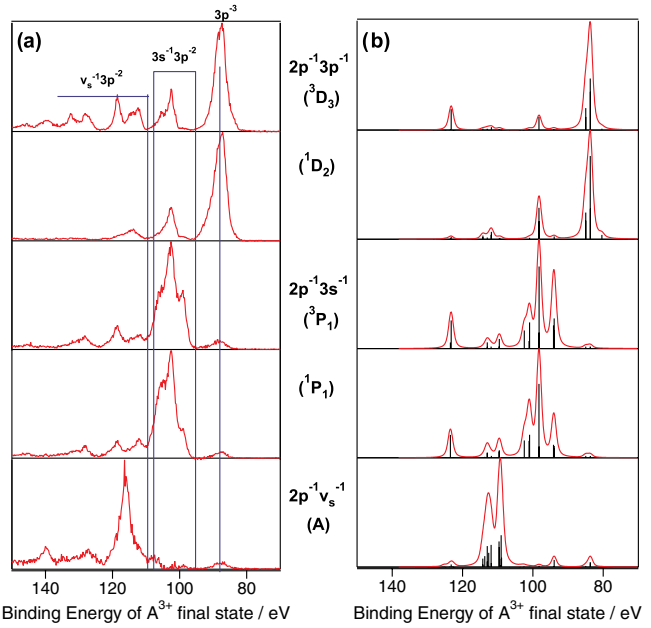

FIG. 3 (color online). Auger spectra associated with the decay of selected Ar^{2+} $2p^{-1}v^{-1}$ states, represented as a function of the binding energy E_b of the final Ar^{3+} states. $E_b = h\nu - (E_{ph1} + E_{ph2} + E_{Auger})$, as deduced from Eq. (1). (a) Experiment from Fig. 2. Three groups of final states are indicated, with configurations $3p^{-3}$, $3s^{-1}3p^{-2}$ and $v_s^{-1}3p^{-2}$. (b) Theory: bars convoluted with 2 eV FWHM Gaussians, to simulate experimental resolution.

individual Ar^{2+} ($2p^{-1}3p^{-1}$) state. The associated lifetime broadenings are too small to be observed in the photoelectron spectrum of Fig. 1(b) where the experimental resolution is of the order of 500 meV. The method to improve energy resolution with our time-of-flight technique is to use lower photon energies providing slower and better resolved photoelectrons. It has the supplementary advantage to induce a strong postcollision interaction (PCI) between the photoelectrons and the Auger electrons, which magnifies the effect of the lifetime broadening. We used photon energies of 292.5 and 320.3 eV to study, respectively, the $2p^{-1}3p^{-1}$ and $2p^{-1}3s^{-1}$ states, as displayed in Fig. 4. It is seen that the relative intensities of the states depend strongly on the photon energy: the Ar^{2+} $2p^{-1}3p^{-1}$ ($^1S_0$) is one of the dominant peak in Fig. 1(b) while it is only weakly populated in Fig. 4. The ratio between the $2p^{-1}3s^{-1}$ and the $2p^{-1}3p^{-1}$ states is also found to diminish strongly from $h\nu = 334.3$ eV [Fig. 1(b)] to 320.3 eV (inset in Fig. 4), passing from 37% to 7%. This evolution reflects the different core valence double ionization mechanisms at play in Eq. (1a): the higher photon energy used in Fig. 1 is above the $2s$ threshold of 326.25 eV [21] and the $2p^{-1}v^{-1}$ states are strongly populated by the resonant contribution of the $2s$ Coster-Kronig decay [11]. On the contrary, at the lower energies of Fig. 4, these states are mainly populated by core valence double ionization, which was shown to be dominantly a direct

TABLE I. Binding energies and lifetime widths of Ar^{2+} $2p^{-1}v^{-1}$ core valence states. Error bars on lifetime widths are estimated to be of ±50%.

Assignment	Theory Energy (eV) [11]	Theory Lifetime width (meV)	Experiment Energy (eV) [11]	This Experiment Energy (Fig. 4)	This Experiment Lifetime width
$2p^{-1}\,3p^{-1}\,(^1P_1)$	276.954	16	⋯	278.52	20
$2p^{-1}\,3p^{-1}\,(^3D_3)$	277.284	10	278.9	278.78	30
$2p^{-1}\,3p^{-1}\,(^3D_2)$	278.149	77	279.9	279.60	80
$2p^{-1}\,3p^{-1}\,(^3S_1)$	278.656	115	279.9	279.96	80
$2p^{-1}\,3p^{-1}\,(^3P_2)$	279.339	438	280.4	280.63	200
$2p^{-1}\,3p^{-1}\,(^3D_1)$	279.693	11	281.2	281.13	15
$2p^{-1}\,3p^{-1}\,(^3P_0)$	280.235	466	282.5	281.32	200
$2p^{-1}\,3p^{-1}\,(^3P_1)$	280.828	346	282.5	281.98	200
$2p^{-1}\,3p^{-1}\,(^1D_2)$	281.721	421	283.3	283.01	200
$2p^{-1}\,3p^{-1}\,(^1S_0)$	283.849	442	285.3	284.97	250
$2p^{-1}\,3s^{-1}\,(^3P_2)$	291.528	176	294.3	294.2	80
$2p^{-1}\,3s^{-1}\,(^3P_1)$	292.142	178	294.9	294.73	200
$2p^{-1}\,3s^{-1}\,(^3P_0)$	293.740	172	⋯	⋯	
$2p^{-1}\,3s^{-1}\,(^1P_1)$	294.273	175	297.0	296.78	200

process, with little contribution of the decay of Ar $2p$ satellite states [22].

Distortion of electron lines due to the postcollision interaction of one photoelectron with one [23] or two

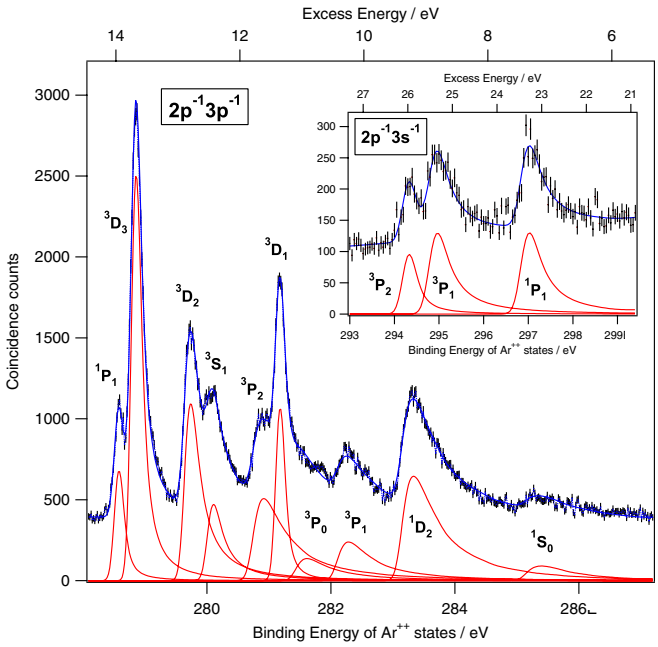

FIG. 4 (color online). Ar^{2+} $2p^{-1}v^{-1}$ states populated by core valence double ionization with photons of 292.5 eV (main frame) and 320.3 eV (insert). The points with error bars give the histogram of the sum of the kinetic energies of the two photoelectrons, when filtered by the simultaneous detection of a 100–200 eV Auger electron. They have been fitted with PCI distorted line shapes which reveal the contributions associated with each Ar^{2+} state -red lines- The theoretical line shapes come from the PCI model developed here and were convoluted with a 150 meV (main frame) or 280 meV (insert) FWHM Gaussian to account for the experimental resolution.

[24] Auger electrons emitted afterwards is well known, but it was not known in the present case where the interaction is between two photoelectrons and one Auger electron emitted afterwards. We have developed a model based on the eikonal approach, which takes into account the interaction between the two photoelectrons, the Auger electron and the ionic field which varies in the course of the Auger decay. This model is an extension of the PCI model used earlier in the processes of the inner shell ionization by electron impact [25]. The PCI distortion factor in our model has a form which is usual for the eikonal approach [23]; it is governed by the width Γ of the $2p^{-1}v^{-1}$ states and the kinematical dimensionless factor $\xi = 1/V_1 + 1/V_2 - 1/V_{13} - 1/V_{23}$ with V_1, V_2, V_3 being the velocities of the two photoelectrons and Auger electron, correspondingly. The positions of unshifted lines and the widths of the calculated line shapes are considered as adjustable parameters of the model. The calculated line shapes were convoluted with a Gaussian to account for the experimental resolution. With the help of this PCI model, it was possible to extract experimental binding energies and lifetimes from the PCI distorted line shapes in Fig. 4. They are reported in Table I. As the model does not provide an analytical formula suitable for a fit procedure, a trial and error method was adopted, with the criterion of minimizing the χ^2 parameter. All the Ar^{2+} $2p^{-1}3p^{-1}$ states are isolated and better positioned than in our previous study [11]. Their lifetime widths are found to agree reasonably well with our calculations. The different lifetime widths result from the general property that the Auger transitions are stronger for the transitions in which the coupling of the individual electrons is preserved. The same effect is observed upon inner-shell ionization of the open shell atoms Sn [26], Al [27], and Cs [28].

Note finally that a number of core valence double photoionization studies have been carried out, since their first detailed investigation with multielectron coincidence techniques [29], both in atoms [30] and in molecules [31–34]; but they have not been interpreted as yielding detailed information on the inner-shell ionization of the associated ions.

In conclusion, a multielectron coincidence experiment, based on core valence double photoionization of the neutral Ar atom, is used to obtain information on the $2p$ inner-shell ionization of an Ar^+ ion. The spectroscopy of the different inner-shell states, their lifetimes, and the Auger spectra associated with their decays are retrieved and found in good agreement with our predictions. This method is expected to lead to important information on the core ionization of singly charged ions, and is expected to be extended to the study of core ionization of doubly charged ions; it will suffice to add a further coincidence degree in order to interpret the already documented core valence triple ionization paths [35]. Direct measurements of photoelectrons and Auger electrons of ionic species will be made more and more possible in the future by free electron laser radiation as a source for multiphoton ionization (see, e.g., Ref. [36]).

Experiments were done with the approval of Advisory Committees: Projects No. 2008-1-70762 in BESSY and No. 2008G529 in PF. The financial support from CNRS (PICS No. 5364) and from the European Community, Research Infrastructure Action under the FP6 "Structuring European research Area" Programme (Contract No. R II 3-CT-2004-506008) are acknowledged. The work has also been supported by the Research Council for Natural Sciences and Engineering of the Academy of Finland. We thank Dr. Kari Jänkälä for helpful discussions.

[1] J. B. West, J. Phys. B **34**, R45 (2001); H. Kjeldsen, J. Phys. B **39** R325 (2006)
[2] A. Müller *et al.*, J. Phys. B **42**, 235602 (2009).
[3] A. Müller, S. Schippers, R. A. Phaneuf, S. W. J. Scully, A. Aguilar, C. Cisneros, M. F. Gharaibeh, A. S. Schlachter, and B. M. McLaughlin, J. Phys. B **43**, 135602 (2010).
[4] M. F. Gharaibeh *et al.*, J. Phys. B **44**, 175208 (2011).
[5] C. Blancard *et al.*, Phys. Rev. A **85**, 043408 (2012).
[6] A. Gottwald, Ch. Gerth, and M. Richter, Phys. Rev. Lett. **82**, 2068 (1999).
[7] J. M. Bizau, D. Cubaynes, M. Richter, F. Wuilleumier, J. Obert, J. Putaux, T. Morgan, E. Källne, S. Sorensen, and A. Damany, Phys. Rev. Lett. **67**, 576 (1991).
[8] S. Al Moussalami, J. Bizau, B. Rouvellou, D. Cubaynes, L. Journel, F. Wuilleumier, J. Obert, J. Putaux, T. Morgan, and M. Richter, Phys. Rev. Lett. **76**, 4496 (1996).
[9] A. Gottwald, S. Anger, J.-M. Bizau, D. Rosenthal, and M. Richter, Phys. Rev. A **55**, 3941 (1997).
[10] F. Penent, P. Lablanquie, J. Palaudoux, L. Andric, G. Gamblin, Y. Hikosaka, K. Ito, and S. Carniato, Phys. Rev. Lett. **106**, 103002 (2011).
[11] P. Lablanquie, S.-M. Huttula, M. Huttula, L. Andric, J. Palaudoux, J. H. D. Eland, Y. Hikosaka, E. Shigemasa, K. Ito, and F. Penent, Phys. Chem. Chem. Phys. **13**, 18 355 (2011).
[12] K. Ito, F. Penent, Y. Hikosaka, E. Shigemasa, I. H. Suzuki, J. H. D. Eland, and P. Lablanquie, Rev. Sci. Instrum. **80**, 123101 (2009), and references therein.
[13] See Supplemental Material at http://link.aps.org/supplemental/10.1103/PhysRevLett.110.113002 for a complete report of all Auger spectra.
[14] T. Kylli, H. Aksela, O.-P. Sairanen, A. Hiltunen, and S. Aksela, J. Phys. B **30**, 3647 (1997).
[15] F. A. Parpia, C. F. Fisher, and I. P. Grant, Comput. Phys. Commun. **94**, 249 (1996).
[16] S. Fritzsche, C. F. Fisher, and G. Gaigalas, Comput. Phys. Commun. **148**, 103 (2002).
[17] G. Gaigalas, T. Zalandauskas, and S. Fritzsche, Comput. Phys. Commun. **157**, 239 (2004).
[18] J. Tulkki, N. M. Kabachnik, and H. Aksela, Phys. Rev. A **48**, 1277 (1993).
[19] S. Fritzsche, Comput. Phys. Commun. **183**, 1525 (2012).
[20] M. Jurvansuu, A. Kivimäki, and S. Aksela, Phys. Rev. A **64**, 012502 (2001).
[21] P. Glans, R. LaVilla, M. Ohno, S. Svensson, G. Bray, N. Wassdahl, and J. Nordgren, Phys. Rev. A **47**, 1539 (1993).
[22] M. Nakano, Y. Hikosaka, P. Lablanquie, F. Penent, S.-M. Huttula, I. H. Suzuki, K. Soejima, N. Kouchi, and K. Ito, Phys. Rev. A **85**, 043405 (2012).
[23] M. Kuchiev and S. Sheinerman, Sov. Phys. JETP **63**, 986 (1986).
[24] S. Sheinerman, P. Lablanquie, F. Penent, Y. Hikosaka, T. Kaneyasu, E. Shigemasa, and K. Ito, J. Phys. B **43**, 115001 (2010).
[25] M. Kuchiev and S. Sheinerman, Sov. Phys. Tech. Phys. **32**, 879 (1987).
[26] M. Huttula, E. Kukk, S. Heinäsmäki, M. Jurvansuu, S. Fritzsche, H. Aksela, and S. Aksela, Phys. Rev. A **69**, 012702 (2004).
[27] K. Jänkälä, S. Fritzsche, M. Huttula, J. Schulz, S. Urpelainen, S. Heinäsmäki, S. Aksela, and H. Aksela, J. Phys. B **40**, 3435 (2007).
[28] L. Partanen, J. Schulz, M. Holappa, H. Aksela, and S. Aksela, Phys. Rev. A **80**, 042518 (2009).
[29] Y. Hikosaka, T. Aoto, P. Lablanquie, F. Penent, E. Shigemasa, and K. Ito, Phys. Rev. Lett. **97**, 053003 (2006).
[30] E. Andersson, P. Linusson, S. Fritzsche, L. Hedin, J. H. D. Eland, L. Karlsson, J.-E. Rubensson, and R. Feifel, Phys. Rev. A **85**, 032502 (2012).
[31] Y. Hikosaka, T. Kaneyasu, E. Shigemasa, P. Lablanquie, F. Penent, and K. Ito, J. Chem. Phys. **127**, 044305 (2007).
[32] T. Kaneyasu, Y. Hikosaka, E. Shigemasa, P. Lablanquie, F. Penent, and K. Ito, J. Phys. B **41**, 135101 (2008).
[33] J. H. D. Eland *et al.*, J. Chem. Phys. **132**, 104311 (2010); **135**, 134309 (2011)
[34] J. Niskanen *et al.*, Phys. Rev. A **82**, 043436 (2010); **85**, 023408 (2012).
[35] Y. Hikosaka, P. Lablanquie, F. Penent, J. Palaudoux, L. Andric, K. Soejima, E. Shigemasa, I. H. Suzuki, M. Nakano, and K. Ito, Phys. Rev. Lett. **107**, 113005 (2011).
[36] M. Braune, A. Reinköster, J. Viefhaus, S. Korica, and U. Becker, J. Phys. Conf. Ser. **194**, 032016 (2009).